ACS Catalysis

Research Article

Cite This: ACS Catal. 2019, 9, 8276−8284

pubs.acs.org/acscatalysis

Electrostatic Effects Accelerate Decatungstate-Catalyzed C−H Fluorination Using [^{18}F]- and [^{19}F]NFSI in Small Molecules and Peptide Mimics

Zheliang Yuan,[†,‡] Hua Yang,[‡] Noeen Malik,[‡] Milena Čolović,[⊥] David S. Weber,[†] Darryl Wilson,[†] François Bénard,[⊥] Rainer E. Martin,[§] Jeffrey J. Warren,[†] Paul Schaffer,[‡] and Robert Britton*[,†]

[†]Department of Chemistry, Simon Fraser University, Burnaby, British Columbia V5A 1S2, Canada

[‡]Life Sciences Division, TRIUMF, Vancouver, British Columbia V6T 2A3, Canada

[§]Medicinal Chemistry, Roche Pharma Research and Early Development (pRED), Roche Innovation Center Basel, F. Hoffmann-La Roche Ltd., Grenzacherstrasse 124, CH-4070 Basel, Switzerland

[⊥]Department of Molecular Oncology, BC Cancer Agency, Vancouver, British Columbia V5Z 1L3, Canada

Supporting Information

ABSTRACT: The site-selective fluorination of unactivated C(sp^3)-H bonds provides unique opportunities to rapidly alter drug properties or generate radiotracers for positron emission tomography (PET) imaging. Toward this goal, photoactivated decatungstate (DT) is capable of generating carbon radicals through hydrogen atom transfer that subsequently undergo fluorination by reaction with *N*-fluorobenzenesulfonimide (NFSI) or [^{18}F]NFSI. This process enables C(sp^3)-H fluorination of a wide range of aliphatic compounds, though reaction rates can be highly variable and limit applications in radiotracer synthesis. Here, we demonstrate that cationic ammonium functions in aliphatic molecules promote formation of a precursor complex with DT that significantly increases the rate of C−H abstraction. The general utility of this rate-accelerating electrostatic effect is demonstrated on more than 30 ammonium-containing molecules, including amino acids, heterocycles, and pseudopeptides. Moreover, this effect is highlighted in the rapid production of [^{18}F]Glu-U-FHLeu, a ^{18}F-labeled prostate specific membrane antigen (PSMA)-binding ligand.

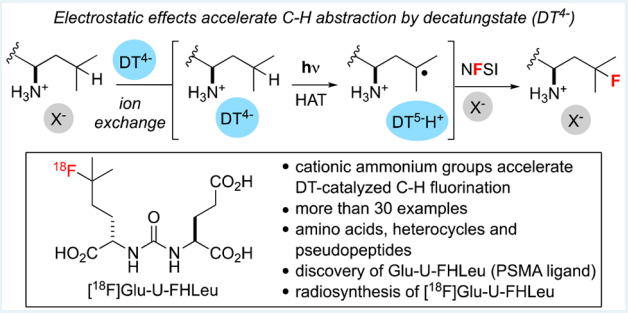

KEYWORDS: *fluorination, decatungstate, photocatalysis, electrostatic effect, PSMA*

INTRODUCTION

Site-selective functionalization of unactivated C(sp^3)−H bonds has become an increasingly common tactic in organic synthesis[1] and provides unique opportunities in medicinal chemistry to rapidly carry out structure−function relationship studies without complicated resynthesis efforts.[2] Among the many C−H functionalization strategies, hydrogen atom transfer (HAT) processes[3] involving photoactivated catalysts[3,4] can provide excellent selectivity based on a combination of substrate and catalyst bias. In this regard, the inexpensive polyoxometalate decatungstate[5] ($W_{10}O_{32}^{4-}$ (DT), Figure 1) has proven to be particularly useful. Near-UV irradiation of DT gives rise to a singlet excited state that quickly decays to a more long-lived reactive intermediate (wO) capable of single electron transfer or HAT from aliphatic compounds.[5,6] Pioneering studies by Hill[5a,7] demonstrated that alkane dehydrogenation,[7c] epimerization,[7a] and carbonylation[7b] can be readily affected using DT catalysis. Fagnoni,[5b,8] Albini,[9] Ravelli,[8d,9] and Ryu[8e,f,j,k] have demonstrated that DT-promoted C(sp^3)−H abstraction can be coupled with several useful C−C, C−Si, and C−N bond-forming reactions. In addition, Noël[10a] and Orfanopolous[10b,c] have studied alkane and alcohol oxidation by photoactivated DT. Recently, a report from Merck highlighted the utility of this catalyst for oxidation of C−H bonds in aliphatic amines,[11] MacMillan reported the coupling of DT catalysis with nickel-mediated cross-coupling reactions to form C−C bonds,[12a] and Melchiorre demonstrated asymmetric conjugate addition of DT-generated carbon radicals.[12b] In work from our laboratories,[13] we paired DT-catalyzed HAT with fluorine atom transfer from *N*-fluorobenzenesulfonimide (NFSI) to affect the direct fluorination of aliphatic[13a,b] and benzylic C−H bonds.[13d] Further, we recently disclosed the direct ^{18}F-fluorination of amino acids[13e,g] and peptides[13f] in aqueous media using DT as a means to generate positron emission tomography (PET) imaging agents for oncology.

Received: May 28, 2019
Revised: July 9, 2019

DOI: 10.1021/acscatal.9b02220
ACS Catal. 2019, 9, 8276−8284

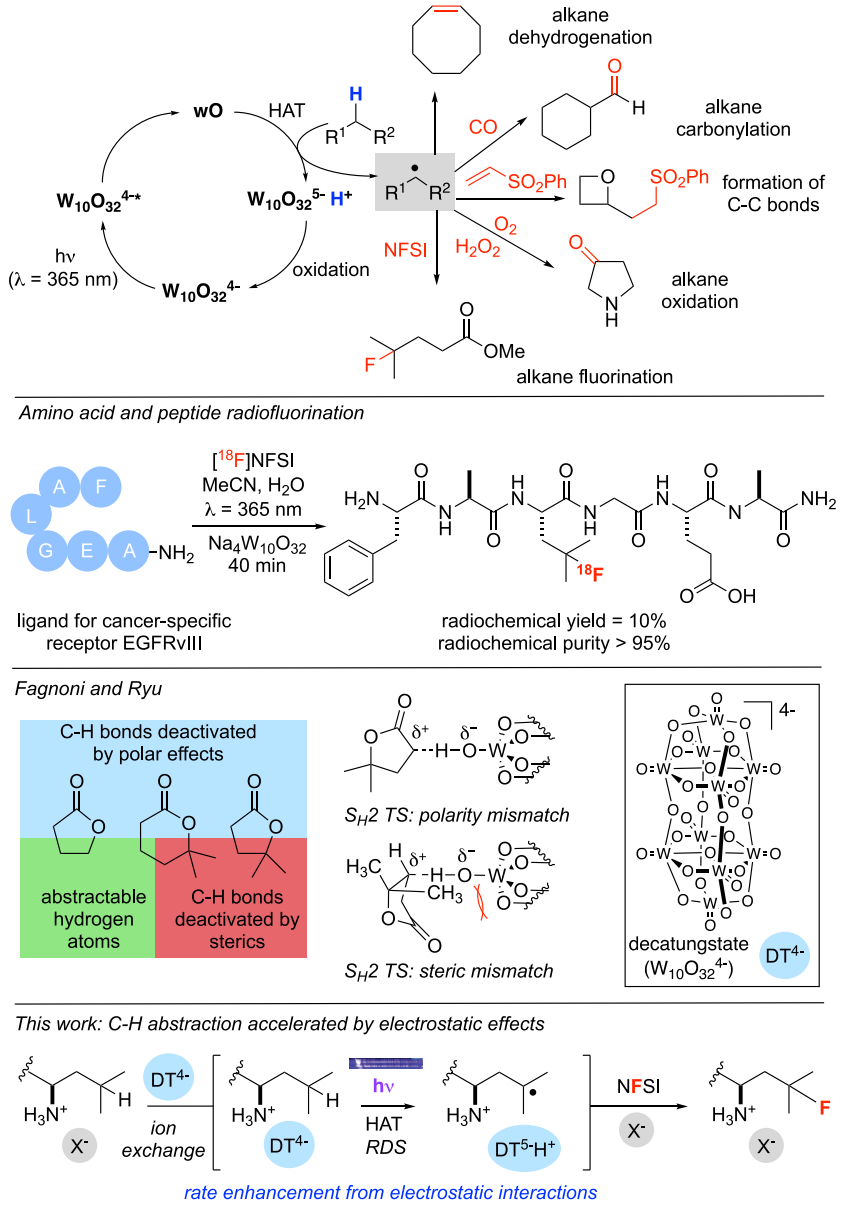

Figure 1. Direct functionalization of unactivated C(sp^3)–H bonds using DT catalysis. Photoactivation of the polyoxometalate DT (DT: $W_{10}O_{32}^{4-}$) produces a reactive intermediate (wO) capable of C–H abstraction from various hydrocarbons. Both steric and polar effects can be exploited for selective HAT to photoexcited DT in lactones and cyclic ketones. Here, we demonstrate that HAT to DT can be greatly accelerated by electrostatic effects in a wide range of substrates.

Despite the many practical applications of DT catalysis in C(sp^3)–H functionalization, subtle substrate structural features often have a significant impact on the rate and productivity of the crucial HAT step, thus complicating widespread application.[14] In an effort to rationalize trends in reactivity and selectivity, Ryu and Fagnoni studied the alkylation of several lactones and cyclic ketones using tetrabutylammonium decatungstate (TBADT).[14c] As summarized in Figure 1, those researchers found that, in addition to C(sp^3)–H bond strength, polar and steric effects govern selectivity in DT-catalyzed HAT.[6,14c] Specifically, they demonstrated that in simple molecules hydrogen atoms remote to quaternary carbons and electron-withdrawing groups were most readily abstracted. During our own studies of DT-catalyzed C–H fluorination,[13a−f] we observed similar trends manifested in the selectivity for fluorination of the γ- or branched position in leucine residues in native peptides.[13f] In that example, the weaker tertiary C–H bond most remote from the sterically hindered and electron-deficient peptide backbone is selected for HAT. However, we have also encountered several reactivity and selectivity trends that require further explanation. For example, the yield and rate of leucine fluorination in native peptides varies significantly depending on neighboring amino acids.[13f] Likewise, γ-fluorination of leucine is much faster than benzylic fluorination[13d] despite a stronger C–H bond. In the present article, we systematically explore an electrostatic rate-accelerating effect on DT-catalyzed HAT (Figure 1, bottom) and exploit this effect in the radiosynthesis of [^{18}F]Glu-U-FHLeu, a potential ^{18}F-labeled tracer for PET imaging of prostate cancer (PCa; FHLeu: 5-fluorohomoleucine).

DOI: 10.1021/acscatal.9b02220
ACS Catal. 2019, 9, 8276–8284

Table 1. DT-Catalyzed C−H Fluorination of Leucine Derivatives[a]

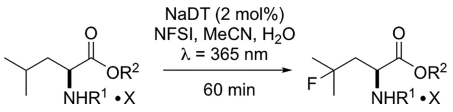

entry	R^1	R^2	X	conv.[b,c]	conv.[b,d]	c log P[e]	$k_{HAT} \times 10^8$ (M^{-1} s^{-1})[f]
1	H	H	TFA	80	91	−1.59 (−1.56)[g]	5.2 ± 0.4
2	H	H	HCl	77	93	−1.59	nd
3	CH_3CO	H		37	34	0.80	1.0 ± 0.1
4	CF_3CO	H		14	9	1.85 (1.89)[g]	nd
5	C_2H_5CO	H		34	30	1.29	nd
6	C_6H_5CO	H		20	18	2.28	nd
7	^{t}BuCO	H		20	18	2.08	nd
8	Boc	H		14	9	2.39	0.30 ± 0.1
9	Ts	H		6	7	2.46	0.35 ± 0.04
10	H	CH_3	HCl	100	100	0.72	6.3 ± 1.0
11	CH_3CO	CH_3		30	37	1.16	2.2 ± 0.2
12	CH_3CO	$(CH_2)_2NH_2$	TFA	74	98	0.18	5.5 ± 1.5
13[h]	H	H	TFA	74	nd	−1.59 (−1.56)[g]	5.2 ± 0.4

[a]nd = not determined. [b]Conversion as a percentage relative to the conversion of leucine methyl ester·HCl (entry 10) after 60 min using the specified reactor configuration (30% conversion in borosilicate NMR tube, 56% conversion in PTFE tube reactor, see the Supporting Information for details). [c]Reaction carried out in a borosilicate NMR tube (see the Supporting Information for details). [d]Reaction carried out in a PTFE tube reactor (see the Supporting Information for details). [e]c log P predictions using KOWWIN v1.57 (Syracuse Research Corporation, New York, USA). [f]Rate constant for C−H abstraction by wO (see the Supporting Information for details). [g]Measured log P values. [h]*N*-fluoro-*N*-(4-(trifluoromethyl)phenyl)benzenesulfonamide used in place of NFSI.

RESULTS AND DISCUSSION

DT-Catalyzed Fluorination of Leucine Derivatives Reveals Electrostatic Effects. As a first step toward gaining additional insight into the effects of substitution and the local environment on the rate and productivity of DT-catalyzed C−H functionalization, we studied the fluorination of several derivatives of leucine, which itself is an excellent substrate. The productivity of fluorination of these derivatives is summarized in Table 1 as a percentage conversion relative to leucine methyl ester·HCl. There was little effect of the counterion on the reaction rate (e.g., entries 1 and 2),[13b] and the productivity of DT-catalyzed fluorination was found to decrease significantly when the amine function was acylated (entries 3−7). For example, the fluorination of trifluoroacetamide or benzamide derivatives of leucine was ∼4−5 times slower than that of the leucine methyl ester·HCl salt (entries 4 and 6). This diminution in rate was also observed for *N*-Boc (entry 8) and the *p*-toluenesulfonamide (entry 9) derivatives. Conversely, the methyl and *t*-butyl (not shown) esters of leucine were excellent substrates for C−H fluorination (e.g., entry 10) except when *N*-acylated (entry 11). This series of experiments suggested that the ammonium function is crucial for rapid fluorination and that substrate hydrophobicity is also linked to fluorination productivity.

To explore the impact of hydrophobicity, the measured partition coefficient (log P) for leucine·TFA (log P = −1.56) and *N*-(trifluoroacetyl)leucine (log P = 1.89) was compared with predicted log P values[15] (c log P = −1.59 and 1.85, respectively). As experimental and calculated log P values matched closely, we opted to calculate log P for the remaining leucine derivatives (Table 1) and found that the most hydrophilic compounds (c log P < 1) were the best substrates for fluorination (e.g., entries 1, 2, 10, and 12). Conversely, lipophilic (c log P > 2) amides, carbamates, and sulfonamides were poor substrates. To probe the importance of a cationic function to DT-catalyzed fluorination, the TFA salt of the ethanolamine ester of *N*-acetyl leucine was prepared and fluorinated under standard conditions (entry 12). This addition of a cationic ammounium function improved the reactivity of *N*-acyl leucine. Here, rapid fluorination with a rate similar to that of leucine·TFA (entry 1) was observed. While c log P values are clearly linked to cationic functions (i.e., charged complexes will have innately higher water solubility), it should be emphasized that compounds with similar c log P values, but with or without charge, have very different fluorination rates (e.g., entries 3 and 10).

We also evaluated the influence of the N−F bond dissociation energy (BDE) of the fluorination reagent on the reaction rate using *N*-fluoro-*N*-(4-(trifluoromethyl)phenyl)-benzenesulfonamide (BDE(N−F) = 222.3 kJ mol^{-1}),[16] an *N*-fluoro-*N*-arylsulfonamide (NFAS) recently reported by Renaud.[16] Although *N*-fluoro-*N*-(4-(trifluoromethyl)phenyl)-benzenesulfonamide has BDE(N−F) ≈ 40 kJ mol^{-1} lower than that in NFSI (BDE(N−F) = 259.3 kJ mol^{-1}), the rate of fluorine atom transfer to carbon radicals is predicted to be faster for NFSI.[16] Here, we observed similar kinetics for both reactions (cf. entries 1 and 13), indicating that C−H abstraction is likely to be rate-limiting in DT-catalyzed fluorination of leucine.

Transient Absorption Spectroscopy. DT is known to activate C−H bonds in aliphatic compounds[17] through a photochemically generated intermediate wO.[18] wO is a powerful oxidant, and many different C−H, N−H, and O−H bonds also can be activated via H-abstraction or outer-sphere electron transfer.[19] The transient spectroscopy of wO is established, and bond activation reactions are readily monitored using the blue absorbance band (λ_{max}= 780 nm) of wO.[18−20] In MeCN solvent, wO decays with a time constant (τ) of about 60 ns in the absence of substrate.[20] For C−H abstraction reactions in MeCN, H• can be removed from aliphatic compounds with rate constants of 10^7−10^8 M^{-1} s^{-1}. In order to compare those data in MeCN with the partially aqueous experiments described here, the reactivity of NaDT in

DOI: 10.1021/acscatal.9b02220
ACS Catal. 2019, 9, 8276−8284

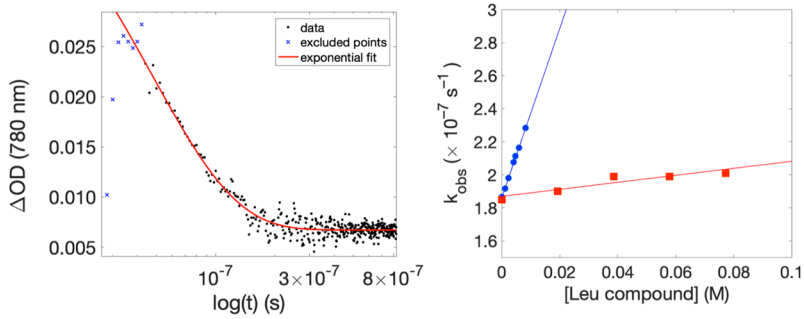

Figure 2. (Left) Example kinetics trace (780 nm) and single-exponential fit for reaction of wO with the TFA salt of leucine. Blue × symbols denote excluded data that are part of the instrument response function. The laser power was 9 mJ/pulse at 355 nm. (Right) Pseudo-first-order plots for reactions of wO and Leu·TFA (blue circles) and *N*-Boc-Leu (red squares). The slopes of the linear fits give the second-order rate constants 5.2 × 10^8 (Leu·TFA) and 3.0 × 10^7 M^{-1} s^{-1}(*N*-Boc-Leu).

MeCN−H_2O (80:20) was investigated. Reactions were pumped with 355 nm light from a Nd:YAG laser (7 ns/pulse, 7−9 mJ/pulse), and transient absorbance traces were monitored at 780 nm. In the absence of substrate, wO decays with τ = 53 ± 3 ns. Under pseudo-first-order conditions using cyclohexane as a substrate, the rate constant for C−H abstraction by wO is 1.0 (±0.1) × 10^8 M^{-1} s^{-1}, about a factor of 3 faster than that in MeCN alone.[20]

Next, the reactions of different leucine derivatives with wO were investigated (Table 1). Typical kinetic traces and pseudo-first-order plots for two leucine derivatives are shown in Figure 2. In general, cationic leucine (e.g., Leu·TFA) had second-order rate constants of ≥5 × 10^8 M^{-1} s^{-1}(entry 1). In contrast, those compounds with protected amines but free carboxylates (entries 3 and 8−9; e.g., *N*-Boc-Leu) have second-order rate constants that are 5−10 times smaller. Leucine in its zwitterionic form (see the Supporting Information) and neutral leucine, where both N and O are protected, have intermediate wO quenching rate constants (e.g., entry 11). All rate constants are summarized in Table 1. Notably, observed rate constants for reactions of different leucine derivatives do not depend strongly on the nature of the N or O substituent. For example, reactions of Leu·HCl salts with wO have about the same yield whether the carboxylic acid is protected or not (entry 10). Introduction of cationic groups also affects the reactivity with wO. For example, incorporation of a cationic (−$OCH_2CH_2NH_2$·TFA) group at the carboxylic function of *N*-acetyl Leu results in an increase in the second-order rate constant for reactions with wO by a factor of ∼5 (cf. entries 3 and 12).

These observed kinetics are consistent with a model where electrostatic interactions between cationic leucine derivatives promote formation of a precursor complex (e.g., eq 1, with Leu·TFA as an example substrate).[21] Irradiation of the precursor complex produces the active oxidant wO, followed by hydrogen abstraction (k_{HAT}) and subsequent fluorination reactions.[21] The remote substitution on the leucine amine function (4 bonds removed from the reactive C−H) is expected to have a small effect on C−H bond strength (∼0.5 kcal mol^{-1}).[22] The observation that different groups substituted at the leucine amine or carboxylate give rise to similar wO quenching rate constants supports this contention. Polar and steric effects have been identified as contributors to selectivity in DT-catalyzed C−H functionalization reactions (see above),[6] but the electrostatic accelerating effect here is distinct. This concept is demonstrated most clearly by the order of magnitude increase in the C−H activation rate constant in *N*-acetyl Leu (a neutral substrate, k_{HAT} = (1.0 ± 0.1) × 10^8 M^{-1} s^{-1}) and *N*-acetyl Leu-O$(CH_2)_2NH_3$·TFA (a cationic substrate, k_{HAT} = (5.5 ± 1.5) × 10^8 M^{-1} s^{-1}) (Table 1, entries 3 and 12).

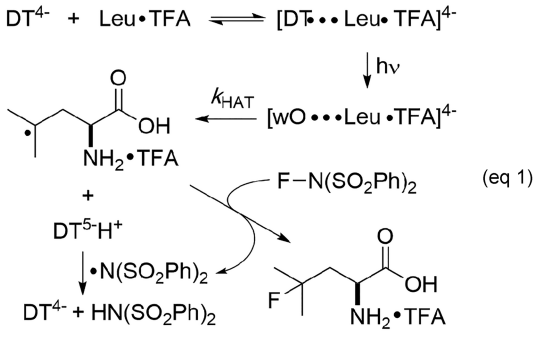

Exploiting Electrostatic Effects for DT-Catalyzed Fluorination. Considering the impressive rate-accelerating electrostatic effect in DT-catalyzed C−H fluorination, the fluorination of several *N*-acyl leucine derivatives that also incorporate an ammonium salt was examined. Remarkably, while fluorination of *N*-acetyl leucine (**1**) proceeded in only 10% yield, after 1 h, the corresponding *N*-glycyl·TFA salt **2** was converted into the fluoroleucine analogue **7** in 61% yield after the same amount of time (Figure 3). Increasing the distance between the ammonium function and site of C−H abstraction had little effect on the reaction yield (e.g., **2**−**5**), although DT-catalyzed fluorination of the TFA salt of the 6-aminohexanoyl ester **5** was complicated by additional fluorination on the side chain itself. Likewise, the fluorination of homoleucine (HLeu)·TFA and 2-amino-6-methylheptanoic acid·TFA provided the corresponding fluorinated adducts **12** and **13** in similar yield (∼50%) after 1 h.[13e,g] Both of these substrates fluorinate faster than leucine·TFA (25% after 1 h) owing to additional separation between the site of C−H abstraction and electron-withdrawing acyl and ammonium functions.[6,13g,14c] To assess whether the rate-accelerating electrostatic effect extends to other aliphatic C−H fluorination reactions, the DT-catalyzed fluorination of *N*-acetyl and *N*-glycyl·TFA derivatives of 2-aminobutane was examined. Again, a distinct increase in product yield was observed for the *N*-glycyl·TFA derivative (cf. **14** and **15**). Likewise, fluorination of O-acetyl-2-hydroxycumene is a nonproductive reaction (∼5% yield), while the O-glycyl·TFA analogue fluorinated with about a 50% yield to

DOI: 10.1021/acscatal.9b02220
ACS Catal. 2019, 9, 8276−8284

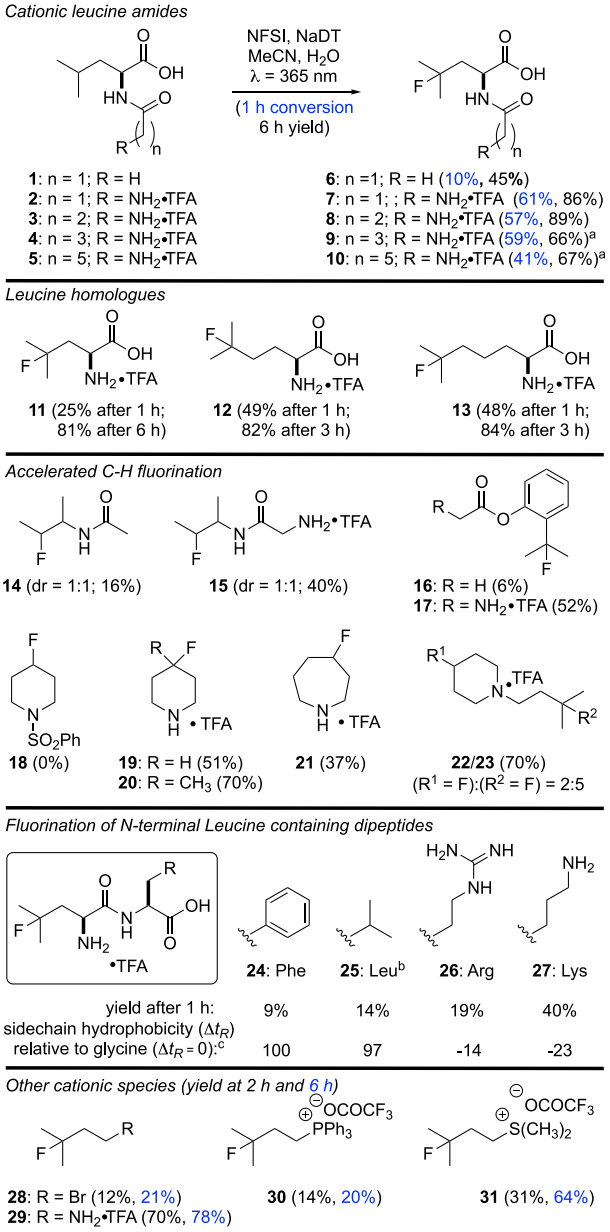

Figure 3. Ammonium-promoted DT-catalyzed C−H fluorination. All reactions were carried out in a custom photobox reactor (see the Supporting Information for details). [a]Accompanied by fluorination on the aliphatic chain; [b]an additional 28% of starting material was fluorinated on the C-terminal leucine residue; [c]side-chain hydrophobicity values from ref 23.

afford **17**. This trend extends to saturated heterocycles, where reaction of *N*-phenylsulfonyl piperidine provided none of the expected 4-fluoro derivative **18** but piperidine·TFA fluorinated cleanly to provide **19** in 51% yield. Although somewhat slower, homopiperidine·TFA could also be fluorinated to provide 4-fluorohomopiperidine (**21**). Introducing a branched position on piperidine (i.e., 4-methylpiperidine) led to further increases in fluorination yield, and 4-methyl-4-fluoropiperidine (**20**) was produced in 70% yield after only 3 h. The reaction of *N*-isopentyl piperidine was examined, and here, the product of tertiary C−H fluorination **23** predominated.

We additionally examined the fluorination of four N-terminal leucine-containing dipeptides: Leu-Phe, Leu-Leu, Leu-Arg, and Leu-Lys. Their fluorination yields after 1 h generally correlate with the additional charge and relative hydrophobicity of the C-terminal amino acid,[13g,23] with C−H fluorination of Leu-Lys being ∼4 times faster than that of Leu-Phe. Interestingly, fluorination of the Leu-Leu dipeptide was complicated by additional fluorination at the C-terminus, which occurred ∼2.5 times faster than that at the N-terminal leucine residue. This latter selectivity is likely derived from the more optimal spacing between the C-terminal branched position and the ammonium function (cf. leucine vs HLeu above).

Finally, the fluorination of other branched alkanes with appended cationic groups was explored. Over the course of 2 h, the triphenylphosphonium salt derived from 3-methyl-1-bromobutane fluorinated with a yield similar to that of the parent bromide (∼10−15%; cf. **28** and **30**), while the fluorinated dimethyl sulfonium salt **31** was produced in ∼30% yield (cf. **28** and **31**). For comparison, the TFA ammonium salt fluorinated cleanly in ∼70% yield after the same reaction time (cf. **28** and **29**). These results are consistent with a model where electrostatic interaction between DT and cationic substrates is the primary determinant of fluorination kinetics. Here, the difference in cation structure (e.g., triphenylphosphonium vs dimethylsulfonium vs ammonium) plays a key role in reaction kinetics as the electrostatic effect associated with precursor complex formation (eq 1) is dependent on $1/r$, where r is the internuclear separation between the cation (substrate) and anion (DT).[21]

Fluorination of ZJ-43: A Potent PSMA Ligand. The prostate specific membrane antigen (PSMA) is a transmembrane protein also known as glutamate carboxypeptidase II (GPCII) that is significantly overexpressed in PCa and linked to both tumor progression and tumorigenesis.[24] The cell surface location and the upregulation in PCa make PSMA an excellent target for molecular imaging by PET.[25] Toward this goal, several classes of PSMA ligands have been identified,[24b] prominent among which are the glutamate/urea-based inhibitors pioneered by Pomper[25] and Kozikowski[26] (e.g., **32**[27] and **33**,[28] Figure 4). A notable requirement for imaging with this family of ligands is a nucleophilic functionality on the nonglutamate residue (e.g., thiol or primary amine) that can be labeled by a radionuclide-containing prosthetic group.[24b] Thus, despite the potent GPCII-inhibitory activity of PSMA-binding ligands such as ZJ-43 (**34**: K_i = 0.8 nM),[29] the lack of a nucleophilic functional group on the leucine residue precludes their investigation as radiotracers for PCa imaging.

We previously reported the direct fluorination of ZJ-43 (**34**)[13f] and found that fluorination occurred cleanly at the branched position of the leucine residue; however, only 7% of the fluorinated derivative (Glu-U-FLeu (**35**); FLeu: 4-fluoroleucine) was produced after 1 h (a relevant time point for radiosyntheses, ^{18}F $t_{1/2}$= 109.8 min). Adjusting the reaction time, equivalents of NFSI, solvent composition, and catalyst loading failed to significantly improve on this result (e.g., 12% after 2 h). Nevertheless, PSMA binding of Glu-U-FLeu (**35**) was evaluated, and this fluorinated derivative was found to retain potent receptor binding (K_i = 1.9 nM). Considering the profound electrostatic effect on the kinetics of DT-catalyzed fluorination described here, the relatively slow fluorination (cf. **11**, Figure 3) of ZJ-43 could now be attributed to the absence of a cationic ammonium function.

This insight prompted a re-examination of the fluorination of several cationic derivatives and analogues of ZJ-43 in an effort to identify a compound that displayed improved

DOI: 10.1021/acscatal.9b02220
ACS Catal. 2019, 9, 8276−8284

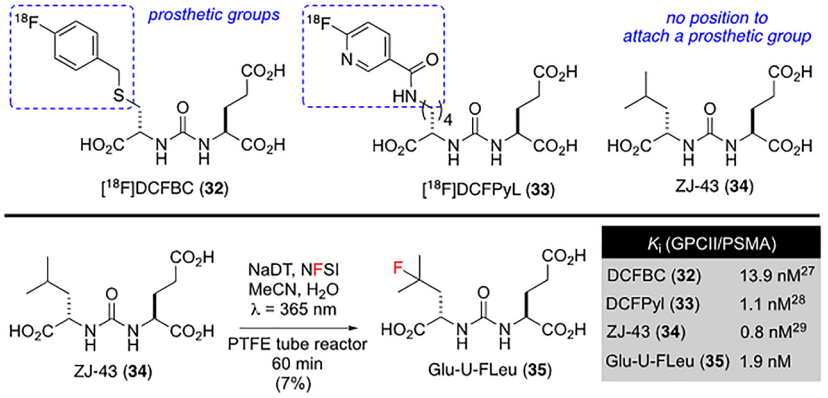

Figure 4. PSMA-binding PET imaging agents [^{18}F]DCFBC and [^{18}F]DCFPyl along with the PSMA ligand ZJ-43. Fluorination of ZJ-43 provides a novel and potent PSMA binding ligand Glu-U-FLeu (**35**) in low yield.

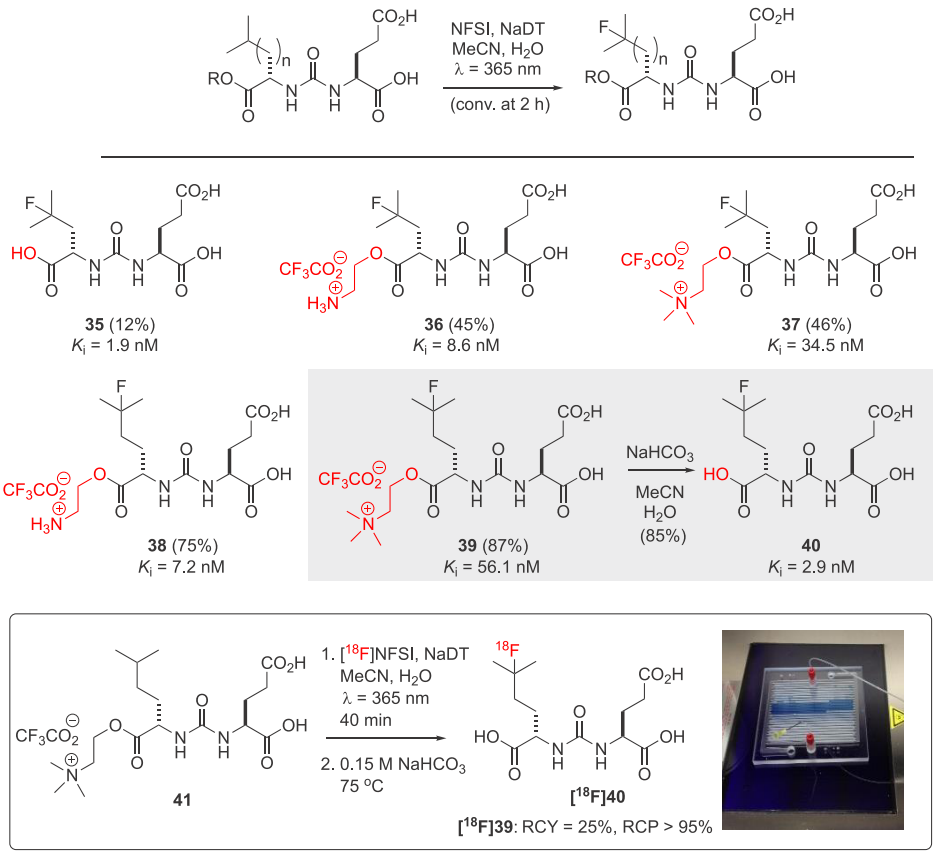

Figure 5. Accelerated fluorination of choline and ethanolamine esters of ZJ-43 and Glu-U-HLeu and synthesis of [^{18}F]Glu-U-FHLeu ([^{18}F]**40**). PSMA binding of each ligand (K_i) was measured by competition assays ($n \geq 3$) using [^{18}F]DCFPyL and determined by applying a one-site Fit K_i model using GraphPad Prism (7.04). ^{19}F-fluorination carried out in a custom photobox reactor and ^{18}F-fluorination carried out in the microreactor depicted placed on top of a transilluminator (see the Supporting Information for full details).

fluorination kinetics and potent PSMA binding (Figure 5). Gratifyingly, the electrostatic effect extended to DT-catalyzed fluorination of both TFA·ethanolamine and choline esters of ZJ-43, both of which fluorinated in ~4-fold improved yield to afford the derivatives **36** and **37**, respectively. Considering that the fluorination of HLeu is more rapid than that of leucine itself (Figure 3),[13e,g] we also explored the DT-catalyzed fluorination of both the TFA·ethanolamine and choline esters of the HLeu analogue of ZJ-43 (Figure 5). Again, both cationic substrates fluorinated cleanly, and adducts **38** and **39** were produced in excellent yield (~80%). Hydrolysis of the choline ester **39** was accomplished by gently warming a solution of this material in MeCN−H_2O with $NaHCO_3$ to provide Glu-U-FHLeu (**40**).

PSMA Binding and Synthesis of [^{18}F]Glu-U-FHLeu. The binding to LNCap PCa cell membranes by each of the fluorinated derivatives **35**−**40** was also evaluated, and the HLeu analogue Glu-U-FHLeu (**40**) proved to be of similar potency to Glu-U-FLeu (**35**). Considering the potential utility of this compound for PET imaging in PCa, we capitalized on the rapid fluorination of the choline ester **41** for the radiosynthesis of [^{18}F]**40** (Figure 5, inset). Using a micro-

DOI: 10.1021/acscatal.9b02220
ACS Catal. 2019, 9, 8276−8284

reactor placed on a transilluminator[13f] and [^{18}F]NFSI,[13e,f,30] the ^{18}F-fluorination of the choline ester proceeded smoothly. Purification of [^{18}F]**39** (along with the remaining starting material) was accomplished by filtration through a strong cation exchange resin, which retained [^{18}F]**39** but not the catalyst, reagents, or byproducts. The purified [^{18}F]**39** was then eluted using aqueous base with >95% radiochemical purity (RCP) and good radiochemical yield (RCY; decay corrected, 25 ± 9%). Hydrolysis of [^{18}F]**39** with heating (75 °C) afforded the triacid [^{18}F]**40**. This synthesis of [^{18}F]Glu-U-FHLeu well demonstrates the practical utility of this electrostatic rate acceleration for DT-catalyzed C−H fluorination.

CONCLUSIONS

The studies described here identify an important electrostatic interaction capable of augmenting the rate of DT-catalyzed C−H fluorination.[31] While such an affect has been hinted at in the literature,[11] this is the first systematic study using a range of small molecules and peptide mimics. Considering the broad and expanding utility of DT-catalyzed C−H functionalization reactions (Figure 1), these results have important implications for both the design and optimization of a wider variety of transformations. In particular, the demonstration that C−H fluorination can be "turned on" for otherwise recalcitrant substrates by simply appending a cationic ammonium function suggests that the scope of late-stage C−H functionalization processes accessible to DT catalysis may be greatly expanded.

Here, we show that several distinct ammonium groups are capable of influencing fluorination kinetics of aliphatic and benzylic C−H bonds in cyclic and acyclic substrates. In addition, dimethylsulfonium cation was demonstrated to improve fluorination reaction rates, though to a lesser degree, while triphenylphosphonium cation has a negligible effect, most likely owing to decreased formation of a cation···DT precursor. Exploiting this electrostatic effect, the fluorination of cationic derivatives of ZJ-43 and Glu-U-HLeu were examined, resulting in the identification of a potent PSMA binding radioligand [^{18}F]Glu-U-FHLeu that could be readily prepared by DT-catalyzed fluorination using [^{18}F]NFSI. These findings add significantly to our understanding of selectivity and reactivity in DT-catalyzed C−H functionalization, and we expect that they will broadly impact the utility and scope of these processes.

ASSOCIATED CONTENT

Supporting Information

The Supporting Information is available free of charge on the ACS Publications website at DOI: 10.1021/acscatal.9b02220.

All experimental procedures and characterization data for new compounds (PDF)

AUTHOR INFORMATION

Corresponding Author

*E-mail: rbritton@sfu.ca.

ORCID

Hua Yang: 0000-0003-1833-9515
François Bénard: 0000-0001-7995-3581
Rainer E. Martin: 0000-0001-7895-497X
Jeffrey J. Warren: 0000-0002-1747-3029
Robert Britton: 0000-0002-9335-0047

Notes

The authors declare no competing financial interest.

ACKNOWLEDGMENTS

We would like to thank Mr. Björn Wagner for measurement of log *P* values. R.B. and J.J.W. acknowledge support from NSERC Discovery Grants, and R.B. acknowledges support from a Michael Smith Foundation for Health Research Career Investigator Award. P.S. acknowledges a Canadian Cancer Society Research Institute Innovation and Innovation to Impact Grant. TRIUMF receives federal funding via a contribution agreement with the National Research Council of Canada.

REFERENCES

(1) (a) Bruckl, T.; Baxter, R. D.; Ishihara, Y.; Baran, P. S. Innate and Guided C-H Functionalization Logic. *Acc. Chem. Res.* **2012**, *45*, 826−839. (b) Gensch, T.; Hopkinson, M. N.; Glorius, F.; Wencel-Delord, J. Mild Metal-Catalyzed C-H Activation: Examples and Concepts. *Chem. Soc. Rev.* **2016**, *45*, 2900−2936. (c) Hartwig, J. F. Evolution of C-H Bond Functionalization from Methane to Methodology. *J. Am. Chem. Soc.* **2016**, *138*, 2. (d) Hartwig, J. F.; Larsen, M. A. Undirected, Homogeneous C-H Bond Functionalization: Challenges and Opportunities. *ACS Cent. Sci.* **2016**, *2*, 281−292. (e) He, J.; Wasa, M.; Chan, K. S. L.; Shao, Q.; Yu, J. Q. Palladium-Catalyzed Transformations of Alkyl C-H Bonds. *Chem. Rev.* **2017**, *117*, 8754−8786. (f) Huang, Z.; Lim, H. N.; Mo, F.; Young, M. C.; Dong, G. Transition Metal-Catalyzed Ketone-Directed or Mediated C-H Functionalization. *Chem. Soc. Rev.* **2015**, *44*, 7764−7786. (g) Roudesly, F.; Oble, J.; Poli, G. Metal-Catalyzed C-H Activation/Functionalization: The Fundamentals. *J. Mol. Catal. A: Chem.* **2017**, *426*, 275−296. (h) Wencel-Delord, J.; Glorius, F. C-H Bond Activation Enables the Rapid Construction and Late-Stage Diversification of Functional Molecules. *Nat. Chem.* **2013**, *5*, 369−375.

(2) Cernak, T.; Dykstra, K. D.; Tyagarajan, S.; Vachal, P.; Krska, S. W. The Medicinal Chemist's Toolbox for Late Stage Functionalization of Drug-like Molecules. *Chem. Soc. Rev.* **2016**, *45*, 546−576.

(3) (a) Capaldo, L.; Ravelli, D. Hydrogen Atom Transfer (HAT): A Versatile Strategy for Substrate Activation in Photocatalyzed Organic Synthesis. *Eur. J. Org. Chem.* **2017**, *2017*, 2056−2071. (b) Protti, S.; Fagnoni, M.; Ravelli, D. Photocatalytic C-H Activation by Hydrogen-Atom Transfer in Synthesis. *ChemCatChem* **2015**, *7*, 1516−1523.

(4) (a) Fagnoni, M.; Dondi, D.; Ravelli, D.; Albini, A. Photocatalysis for the Formation of the C-C Bond. *Chem. Rev.* **2007**, *107*, 2725−2756. (b) Ravelli, D.; Fagnoni, M.; Albini, A. Photoorganocatalysis. What For? *Chem. Soc. Rev.* **2013**, *42*, 97−113. (c) Shi, L.; Xia, W. Photoredox Functionalization of C-H Bonds Adjacent to a Nitrogen Atom. *Chem. Soc. Rev.* **2012**, *41*, 7687−7697.

(5) (a) Hill, C. L. Introduction of Functionality into Unactivated Carbon-Hydrogen Bonds - Catalytic Generation and Nonconventional Utilization of Organic Radicals. *Synlett* **1995**, *1995*, 127−132. (b) Ravelli, D.; Protti, S.; Fagnoni, M. Decatungstate Anion for Photocatalyzed "Window Ledge" Reactions. *Acc. Chem. Res.* **2016**, *49*, 2232−2242. (c) Tanielian, C. Decatungstate Photocatalysis. *Coord. Chem. Rev.* **1998**, *178*−*180*, 1165−1181. (d) Tzirakis, M. D.; Lykakis, I. N.; Orfanopoulos, M. Decatungstate as an Efficient Photocatalyst in Organic Chemistry. *Chem. Soc. Rev.* **2009**, *38*, 2609−2621.

(6) Ravelli, D.; Fagnoni, M.; Fukuyama, T.; Nishikawa, T.; Ryu, I. Site-Selective C-H Functionalization by Decatungstate Anion Photocatalysis: Synergistic Control by Polar and Steric Effects Expands the Reaction Scope. *ACS Catal.* **2018**, *8*, 701−713.

(7) (a) Combs-Walker, L. A.; Hill, C. L. Use of Excited-State and Ground-State Redox Properties of Polyoxometalates for Selective Transformation of Unactivated Carbon-Hydrogen Centers Remote from the Functional Group in Ketones. *J. Am. Chem. Soc.* **1992**, *114*, 938−946. (b) Jaynes, B. S.; Hill, C. L. Radical Carbonylation of Alkanes via Polyoxotungstate Photocatalysis. *J. Am. Chem. Soc.* **1995**,

DOI: 10.1021/acscatal.9b02220
ACS Catal. 2019, 9, 8276−8284

117, 4704−4705. (c) Renneke, R. F.; Pasquali, M.; Hill, C. L. Polyoxometalate Systems for the Catalytic Selective Production of Nonthermodynamic Alkenes from Alkanes. Nature of Excited-State Deactivation Processes and Control of Subsequent Thermal Processes in Polyoxometalate Photoredox Chemistry. *J. Am. Chem. Soc.* **1990**, *112*, 6585−6594.

(8) (a) Esposti, S.; Dondi, D.; Fagnoni, M.; Albini, A. Acylation of Electrophilic Olefins through Decatungstate-Photocatalyzed Activation of Aldehydes. *Angew. Chem., Int. Ed.* **2007**, *46*, 2531−2534. (b) Montanaro, S.; Ravelli, D.; Merli, D.; Fagnoni, M.; Albini, A. Decatungstate as Photoredox Catalyst: Benzylation of Electron-Poor Olefins. *Org. Lett.* **2012**, *14*, 4218−4221. (c) Protti, S.; Ravelli, D.; Fagnoni, M.; Albini, A. Solar Light-Driven Photocatalyzed Alkylations. Chemistry on the Window Ledge. *Chem. Commun.* **2009**, 7351−7353. (d) Qrareya, H.; Dondi, D.; Ravelli, D.; Fagnoni, M. Decatungstate-Photocatalyzed Si-H/C-H Activation in Silyl Hydrides: Hydrosilylation of Electron-Poor Alkenes. *ChemCatChem* **2015**, *7*, 3350−3357. (e) Ryu, I.; Tani, A.; Fukuyama, T.; Ravelli, D.; Fagnoni, M.; Albini, A. Atom-Economical Synthesis of Unsymmetrical Ketones through Photocatalyzed C-H Activation of Alkanes and Coupling with CO and Electrophilic Alkenes. *Angew. Chem., Int. Ed.* **2011**, *50*, 1869−1872. (f) Ryu, I.; Tani, A.; Fukuyama, T.; Ravelli, D.; Montanaro, S.; Fagnoni, M. Efficient C-H/C-N and C-H/C-CO-N Conversion via Decatungstate-Photoinduced Alkylation of Diisopropyl Azodicarboxylate. *Org. Lett.* **2013**, *15*, 2554−2557. (g) Bonassi, F.; Ravelli, D.; Protti, S.; Fagnoni, M. Decatungstate Photocatalyzed Acylations and Alkylations in Flow via Hydrogen Atom Transfer. *Adv. Synth. Catal.* **2015**, *357*, 3687−3695. (h) Capaldo, L.; Fagnoni, M.; Ravelli, D. Vinylpyridines as Building Blocks for the Photocatalyzed Synthesis of Alkylpyridines. *Chem. - Eur. J.* **2017**, *23*, 6527−6530. (i) Corsico, S.; Fagnoni, M.; Ravelli, D. Sunlight Decatungstate Photoinduced Trifluoromethylations of (Hetero)aromatics and Electron-Poor Olefins. *Photochem. Photobiol. Sci.* **2017**, *16*, 1375−1380. (j) Fukuyama, T.; Nishikawa, T.; Yamada, K.; Ravelli, D.; Fagnoni, M.; Ryu, I. Photocatalyzed Site-Selective C(sp^3)-H Functionalization of Alkylpyridines at Non-Benzylic Positions. *Org. Lett.* **2017**, *19*, 6436−6439. (k) Quattrini, M. C.; Fujii, S.; Yamada, K.; Fukuyama, T.; Ravelli, D.; Fagnoni, M.; Ryu, I. Versatile Cross-Dehydrogenative Coupling of Heteroaromatics and Hydrogen Donors via Decatungstate Photocatalysis. *Chem. Commun.* **2017**, *53*, 2335−2338. (l) Ravelli, D.; Zoccolillo, M.; Mella, M.; Fagnoni, M. Photocatalytic Synthesis of Oxetane Derivatives by Selective C-H Activation. *Adv. Synth. Catal.* **2014**, *356*, 2781−2786.

(9) Qrareya, H.; Ravelli, D.; Fagnoni, M.; Albini, A. Decatungstate Photocatalyzed Benzylation of Alkenes with Alkylaromatics. *Adv. Synth. Catal.* **2013**, *355*, 2891−2899.

(10) (a) Laudadio, G.; Govaerts, S.; Wang, Y.; Ravelli, D.; Koolman, H. F.; Fagnoni, M.; Djuric, S. W.; Noel, T. Selective C(sp^3)-H Aerobic Oxidation Enabled by Decatungstate Photocatalysis in Flow. *Angew. Chem., Int. Ed.* **2018**, *57*, 4078−4082. (b) Lykakis, I. N.; Orfanopoulos, M. Photooxidation of Aryl Alkanes by a Decatungstate/Triethylsilane System in the Presence of Molecular Oxygen. *Tetrahedron Lett.* **2004**, *45*, 7645−7649. (c) Lykakis, I. N.; Vougioukalakis, G. C.; Orfanopoulos, M. Homogeneous Decatungstate-Catalyzed Photooxygenation of Tetrasubstituted Alkenes: A Deuterium Kinetic Isotope Effect Study. *J. Org. Chem.* **2006**, *71*, 8740−8747.

(11) Schultz, D. M.; Levesque, F.; DiRocco, D. A.; Reibarkh, M.; Ji, Y. N.; Joyce, L. A.; Dropinski, J. F.; Sheng, H. M.; Sherry, B. D.; Davies, I. W. Oxyfunctionalization of the Remote C-H Bonds of Aliphatic Amines by Decatungstate Photocatalysis. *Angew. Chem., Int. Ed.* **2017**, *56*, 15274−15278.

(12) (a) Perry, I. B.; Brewer, T. F.; Sarver, P. J.; Schultz, D. M.; DiRocco, D. A.; MacMillan, D. W. C. Direct Arylation of Strong Aliphatic C−H Bonds. *Nature* **2018**, *560*, 70−75. (b) Murphy, J. J.; Bastida, D.; Paria, S.; Fagnoni, M.; Melchiorre, P. Asymmetric Catalytic Formation of Quaternary Carbons by Iminium Ion Trapping of Radicals. *Nature* **2016**, *532*, 218−222.

(13) (a) Halperin, S. D.; Fan, H.; Chang, S.; Martin, R. E.; Britton, R. A Convenient Photocatalytic Fluorination of Unactivated C-H Bonds. *Angew. Chem., Int. Ed.* **2014**, *53*, 4690−4693. (b) Halperin, S. D.; Kwon, D.; Holmes, M.; Regalado, E. L.; Campeau, L. C.; DiRocco, D. A.; Britton, R. Development of a Direct Photocatalytic C-H Fluorination for the Preparative Synthesis of Odanacatib. *Org. Lett.* **2015**, *17*, 5200−5203. (c) Meanwell, M.; Lehmann, J.; Eichenberger, M.; Martin, R. E.; Britton, R. Synthesis of Acyl Fluorides via Photocatalytic Fluorination of Aldehydic C-H Bonds. *Chem. Commun.* **2018**, *54*, 9985−9988. (d) Nodwell, M. B.; Bagai, A.; Halperin, S. D.; Martin, R. E.; Knust, H.; Britton, R. Direct Photocatalytic Fluorination of Benzylic C-H Bonds with *N*-Fluorobenzenesulfonimide. *Chem. Commun.* **2015**, *51*, 11783−11786. (e) Nodwell, M. B.; Yang, H.; Colovic, M.; Yuan, Z.; Merkens, H.; Martin, R. E.; Benard, F.; Schaffer, P.; Britton, R. ^{18}F-Fluorination of Unactivated C-H Bonds in Branched Aliphatic Amino Acids: Direct Synthesis of Oncological Positron Emission Tomography Imaging Agents. *J. Am. Chem. Soc.* **2017**, *139*, 3595−3598. (f) Yuan, Z.; Nodwell, M. B.; Yang, H.; Malik, N.; Merkens, H.; Benard, F.; Martin, R. E.; Schaffer, P.; Britton, R. Site-Selective, Late-Stage C-H ^{18}F-Fluorination on Unprotected Peptides for Positron Emission Tomography Imaging. *Angew. Chem., Int. Ed.* **2018**, *57*, 12733−12736. (g) Nodwell, M. B.; Yang, H.; Merkens, H.; Malik, N.; Colovic, M.; Björn, W.; Martin, R. E.; Benard, F.; Schaffer, P.; Britton, R. 18 F-Branched Chain Amino Acids: Structure-Activity Relationships and PET Imaging Potential. *J. Nucl. Med.* **2019**, *60*, 1003−1009.

(14) (a) Fukuyama, T.; Yamada, K.; Nishikawa, T.; Ravelli, D.; Fagnoni, M.; Ryu, I. Site-selectivity in TBADT-photocatalyzed C(sp^3)−H Functionalization of Saturated Alcohols and Alkanes. *Chem. Lett.* **2018**, *47*, 207−209. (b) Waele, V. D.; Poizat, O.; Fagnoni, M.; Bagno, A.; Ravelli, D. Unraveling the Key Features of the Reactive State of Decatungstate Anion in Hydrogen Atom Transfer (HAT) Photocatalysis. *ACS Catal.* **2016**, *6*, 7174−7182. (c) Yamada, K.; Fukuyama, T.; Fujii, S.; Ravelli, D.; Fagnoni, M.; Ryu, I. Cooperative Polar/Steric Strategy in Achieving Site-Selective Photocatalyzed C(sp^3)-H Functionalization. *Chem. - Eur. J.* **2017**, *23*, 8615−8618.

(15) Meylan, W. M.; Howard, P. H. Atom/Fragment Contribution Method for Estimating Octanol-Water Partition Coefficients. *J. Pharm. Sci.* **1995**, *84*, 83−92.

(16) Meyer, D.; Jangra, H.; Walther, F.; Zipse, H.; Renaud, P. A Third Generation of Radical Fluorinating Agents Based on *N*-Fluoro-*N*-arylsulfonamides. *Nat. Commun.* **2018**, *9*, 4888.

(17) (a) Renneke, R. F.; Hill, C. L. Homogeneous Catalytic Photochemical Functionalization of Alkanes by Polyoxometalates. *J. Am. Chem. Soc.* **1986**, *108*, 3528−3529. (b) Hill, C. L.; Prosser-McCartha, C. M. Homogeneous Catalysis by Transition Metal Oxygen Anion Clusters. *Coord. Chem. Rev.* **1995**, *143*, 407−455. (c) Ermolenko, L. P.; Delaire, J. A.; Giannotti, C. Laser Flash Photolysis Study of the Mechanism of Photooxidation of Alkanes Catalysed by Decatungstate Anion. *J. Chem. Soc., Perkin Trans. 2* **1997**, *2*, 25−30.

(18) (a) Duncan, D. C.; Netzel, T. L.; Hill, C. L. Early-Time Dynamics and Reactivity of Polyoxometalate Excited States. Identification of a Short-Lived LMCT Excited State and a Reactive Long-Lived Charge-Transfer Intermediate following Picosecond Flash Excitation of $[W_{10}O_{32}]^{4-}$ in Acetonitrile. *Inorg. Chem.* **1995**, *34*, 4640−4646. (b) Tanielian, C.; Duffy, K.; Jones, A. Kinetic and Mechanistic Aspects of Photocatalysis by Polyoxotungstates: A Laser Flash Photolysis, Pulse Radiolysis, and Continuous Photolysis Study. *J. Phys. Chem. B* **1997**, *101*, 4276−4282.

(19) (a) Texier, I.; Delaire, J. A.; Giannotti, C. Reactivity of the Charge Transfer Excited State of Sodium Decatungstate at the Nanosecond Time Scale. *Phys. Chem. Chem. Phys.* **2000**, *2*, 1205−1212. (b) Lykakis, I. N.; Tanielian, C.; Orfanopoulos, M. Decatungstate Photocatalyzed Oxidation of Aryl Alkanols. Electron Transfer or Hydrogen Abstraction Mechanism? *Org. Lett.* **2003**, *5*, 2875−2878.

DOI: 10.1021/acscatal.9b02220
ACS Catal. 2019, 9, 8276−8284

(20) Duncan, D. C.; Fox, M. A. Early Events in Decatungstate Photocatalyzed Oxidations: A Nanosecond Laser Transient Absorbance Reinvestigation. *J. Phys. Chem. A* **1998**, *102*, 4559−4567.
(21) Eberson, L. In *Advances in Physical Organic Chemistry*; Gold, V., Bethell, D., Eds.l Academic Press, 1982; Vol. *18*, pp 79−185.
(22) (a) McMillen, D. F.; Golden, D. M. Hydrocarbon Bond Dissociation Energies. *Annu. Rev. Phys. Chem.* **1982**, *33*, 493−532. (b) Blanksby, S. J.; Ellison, G. B. Bond Dissociation Energies of Organic Molecules. *Acc. Chem. Res.* **2003**, *36*, 255−263.
(23) Monera, O. D.; Sereda, T. J.; Zhou, N. E.; Kay, C. M.; Hodges, R. S. Relationship of Sidechain Hydrophobicity and Alpha-Helical Propensity on the Stability of the Single-Stranded Amphipathic Alpha-Helix. *J. Pept. Sci.* **1995**, *1*, 319−329.
(24) (a) Evans, J. C.; Malhotra, M.; Cryan, J. F.; O'Driscoll, C. M. The Therapeutic and Diagnostic Potential of the Prostate Specific Membrane Antigen/Glutamate Carboxypeptidase II (PSMA/GCPII) in Cancer and Neurological Disease. *Br. J. Pharmacol.* **2016**, *173*, 3041−3079. (b) Zhou, J.; Neale, J. H.; Pomper, M. G.; Kozikowski, A. P. NAAG Peptidase Inhibitors and Their Potential for Diagnosis and Therapy. *Nat. Rev. Drug Discovery* **2005**, *4*, 1015−1026.
(25) (a) Foss, C. A.; Mease, R. C.; Fan, H.; Wang, Y.; Ravert, H. T.; Dannals, R. F.; Olszewski, R. T.; Heston, W. D.; Kozikowski, A. P.; Pomper, M. G. Radiolabeled Small-Molecule Ligands for Prostate-Specific Membrane Antigen: *in Vivo* Imaging in Experimental Models of Prostate Cancer. *Clin. Cancer Res.* **2005**, *11*, 4022−4028. (b) Mease, R. C.; Foss, C. A.; Pomper, M. G. PET Imaging in Prostate Cancer: Focus on Prostate-Specific Membrane Antigen. *Curr. Top. Med. Chem.* **2013**, *13*, 951−962.
(26) (a) Kozikowski, A. P.; Nan, F.; Conti, P.; Zhang, J.; Ramadan, E.; Bzdega, T.; Wroblewska, B.; Neale, J. H.; Pshenichkin, S.; Wroblewski, J. T. Design of Remarkably Simple, yet Potent Urea-Based Inhibitors of Glutamate Carboxypeptidase II (NAALADase). *J. Med. Chem.* **2001**, *44*, 298−301. (b) Kozikowski, A. P.; Zhang, J.; Nan, F.; Petukhov, P. A.; Grajkowska, E.; Wroblewski, J. T.; Yamamoto, T.; Bzdega, T.; Wroblewska, B.; Neale, J. H. Synthesis of Urea-Based Inhibitors as Active Site Probes of Glutamate Carboxypeptidase II: Efficacy as Analgesic Agents. *J. Med. Chem.* **2004**, *47*, 1729−1738. (c) Nan, F.; Bzdega, T.; Pshenichkin, S.; Wroblewski, J. T.; Wroblewska, B.; Neale, J. H.; Kozikowski, A. P. Dual Function Glutamate-Related Ligands: Discovery of a Novel, Potent Inhibitor of Glutamate Carboxypeptidase II Possessing mGluR3 Agonist Activity. *J. Med. Chem.* **2000**, *43*, 772−774.
(27) Mease, R. C.; Dusich, C. L.; Foss, C. A.; Ravert, H. T.; Dannals, R. F.; Seidel, J.; Prideaux, A.; Fox, J. J.; Sgouros, G.; Kozikowski, A. P.; Pomper, M. G. *N*-[*N*-[(*S*)-1,3-Dicarboxypropyl]Carbamoyl]-4-[^{18}F]-Fluorobenzyl-L-Cysteine, [^{18}F]DCFBC: A New Imaging Probe for Prostate Cancer. *Clin. Cancer Res.* **2008**, *14*, 3036−3043.
(28) Chen, Y.; Pullambhatla, M.; Foss, C. A.; Byun, Y.; Nimmagadda, S.; Senthamizhchelvan, S.; Sgouros, G.; Mease, R. C.; Pomper, M. G. 2-(3- -Ureido)-Pentanedioic Acid, [^{18}F]DCFPyL, a PSMA-Based PET Imaging Agent for Prostate Cancer. *Clin. Cancer Res.* **2011**, *17*, 7645−7653.
(29) Olszewski, R. T.; Bukhari, N.; Zhou, J.; Kozikowski, A. P.; Wroblewski, J. T.; Shamimi-Noori, S.; Wroblewska, B.; Bzdega, T.; Vicini, S.; Barton, F. B.; Neale, J. H. NAAG Peptidase Inhibition Reduces Locomotor Activity and Some Stereotypes in the PCP Model of Schizophrenia via Group II mGluR. *J. Neurochem.* **2004**, *89*, 876−885.
(30) Teare, H.; Robins, E. G.; Arstad, E.; Luthra, S. K.; Gouverneur, V. Synthesis and Reactivity of [F-18]-*N*-fluorobenzenesulfonimide. *Chem. Commun.* **2007**, 2330−2332.
(31) For a recent perspective on exploiting non-covalent interactions in catalysis, see: Davis, H. J.; Phipps, R. J. Harnessing Non-Covalent Interactions to Exert Control Over Regioselectivity and Site-Selectivity in Catalytic Reactions. *Chem. Sci.* **2017**, *8*, 864−877.

DOI: 10.1021/acscatal.9b02220
ACS Catal. 2019, 9, 8276−8284